View metadata, citation and similar papers at core.ac.uk
brought to you by CORE
provided by DSpace@MIT

A CUMULATIVE MIGRATION METHOD FOR COMPUTING RIGOROUS TRANSPORT CROSS SECTIONS AND DIFFUSION COEFFICIENTS FOR LWR LATTICES WITH MONTE CARLO

Zhaoyuan Liu, Kord Smith and Benoit Forget
Department of Nuclear Science and Engineering
Massachusetts Institute of Technology, Cambridge, Massachusetts, USA
liuzy@mit.edu, kord@mit.edu, bforget@mit.edu

Javier Ortensi
Idaho National Laboratory, Idaho Falls, Idaho, USA
javier.ortensi@inl.gov

ABSTRACT

A new method for computing homogenized assembly neutron transport cross sections and diffusion coefficients that is both rigorous and computationally efficient is proposed in this paper. In the limit of a homogeneous hydrogen slab, the new method is equivalent to the long-used, and only-recently-published CASMO transport method. The rigorous method is used to demonstrate the sources of inaccuracy in the commonly applied "out-scatter" transport correction. It is also demonstrated that the newly developed method is directly applicable to lattice calculations performed by Monte Carlo and is capable of computing rigorous homogenized transport cross sections for arbitrarily heterogeneous lattices. Comparisons of several common transport cross section approximations are presented for a simple problem of infinite medium hydrogen. The new method has also been applied in computing 2-group diffusion data for an actual PWR lattice from BEAVRS benchmark.

Key Words: **Transport Cross Section, Diffusion Coefficient, Transport Correction, Monte Carlo, Cumulative Migration Area**

1. INTRODUCTION

Many deterministic nuclear reactor calculations utilize transport-corrected-P_0 transport or diffusion theory to model neutron transport within fuel assemblies and nearby reflecting regions. The accuracy of such core models is inherently tied to approximations made in obtaining multi-group transport cross sections or diffusion coefficients. While classic reactor physics textbooks [1, 2] offer insights and plausible arguments for computing transport cross sections and diffusion coefficients, there appears to be no rigorous theory for, nor quantification of errors introduced by, these approximations. Consequently, the computational accuracy of both heterogeneous (e.g. explicit fuel pin) and nodal (e.g. homogenized

fuel assemblies) core calculations is often seriously compromised by inaccurate transport approximations, and little guidance is available in the literature to assist code developers and analysts in choosing the appropriate transport approximation.

1.1. Background

The generation of multi-group cross section data for LWR analysis usually starts by identifying some characteristic "lattice" — be it a pin-cell, a fuel assembly, or a collection of fuel assemblies. For each such lattice, a very-fine-group transport calculation (e.g., 50 – 10,000 groups) is performed to obtain the neutron flux and reaction rate distributions within the lattice. Unless this transport calculation explicitly models anisotropic scattering, an approximation for transport-corrected-P_0 cross sections for each nuclide must be introduced before the multi-group lattice transport calculation can be performed.

In addition, lattice reaction rates and fluxes are used to compute energy-condensed and/or spatially-homogenized transport cross sections (or diffusion coefficients) for use in downstream multi-group (e.g., 2 – 100 groups) core calculations. Here, additional approximations are required to compute the appropriate transport cross section that preserves some selected characteristic of the lattice calculation.

All production lattice physics codes [3–6] make such approximations, often without substantial justification. Moreover, the most useful of these approximations are often considered to be proprietary, and the literature remains largely silent on useful methods. One example might be that of the transport-corrected-P_0 methods that have been employed in CASMO for more than 40 years. Only recently has Herman [7] published details of the method used in CASMO to generate transport-corrected-P_0 cross sections for ^{1}H in LWR lattices. Herman was able to compute CASMO's "exact" transport cross section that matched continuous-energy Monte Carlo (MC) neutron leakages (integrated into 70 fine energy groups) from a slab of pure hydrogen. This transport correction is markedly different from that computed using the "micro-balance" argument [8] which produces the classic "out-scatter" approximation — with its transport-to-total ratio of 1/3 for purely isotropic center-of-mass neutron scattering with free gas ^{1}H model. CASMO developers recognized long ago that this definition of transport cross section produced excellent eigenvalues for small LWR critical assemblies with large neutron leakages, while the classic out-scatter approximation produced errors in eigenvalue as large as 1000 pcm. In addition, SIMULATE-3 nodal code developers observed (more than 30 years ago) that the CASMO transport cross section also produced two-group diffusion coefficients that eliminated radial power tilts observed in large 4-loop PWR cores when using the out-scatter approximation.

1.2. Approximation Methods For Transport Cross Sections

Many approximation methods for computing diffusion coefficients has been investigated in the past 40 years, among which the "out-scatter" approximation based on the "micro-balance" argument is probably the most often used one, assuming that the in-scatter rate of neutrons from energies E' to E will

approximately balance the out-scatter rate of neutrons from E to all other energies. The approximation can be represented as

$$\int_0^\infty \Sigma_{s1}(\vec{r}, E' \to E)\vec{J}(\vec{r}, E')dE' \approx \int_0^\infty \Sigma_{s1}(\vec{r}, E \to E')\vec{J}(\vec{r}, E)dE' \tag{1}$$

in which $\Sigma_{s1}(\vec{r}, E' \to E)$ is P_1 scattering cross section from E' to E at $\vec{r}$, and $\vec{J}(\vec{r}, E')$ is the neutron current of energy E' at $\vec{r}$. Based on this approximation, the multi-group transport cross section can be derived to be the expression in Equation (2).

$$\Sigma_{tr,g}^{os} = \Sigma_{t,g} - \overline{\mu}_g \Sigma_{s0,g} \tag{2}$$

In the above equation, $\Sigma_{tr,g}^{os}$ is the transport cross section from the out-scatter approximation, $\Sigma_{t,g}$ is total cross section, $\Sigma_{s0,g}$ is P_0 scattering cross section, $\overline{\mu}_g$ is the average scattering cosine of neutron, and all the subscript g denotes the group index. The spatial dependence on $\vec{r}$ is omitted in most equations in this paper for a clearer expression and generally all the terms refer to the same spatial position.

Since in the perspective of neutrons in nuclear reactor physics, the elastic scattering with ^{1}H can be seen as purely isotropic in center-of-mass system, $\overline{\mu}_g$ can be calculated to be $2/3$ when thermalization is not taken into account. This induced an easier way of computing diffusion coefficients by taking $\overline{\mu}_g$ to be $2/3$ for all groups, which can be shown as

$$\Sigma_{tr,g}^{as} = \Sigma_{t,g} - \frac{2}{3}\Sigma_{s0,g} \tag{3}$$

in which $\Sigma_{tr,g}^{as}$ is the transport cross section from the "asymptotic" out-scatter approximation.

Another approximation method makes the hypothesis that neutron current can not exceed the scalar flux and it uses scalar flux spectrum instead of neutron current spectrum for weighting P_1 scattering cross sections [9]. The transport cross section computed by this method as shown in Equation (4) can be called "flux-limited" transport cross section.

$$\Sigma_{tr,g}^{fl} = \Sigma_{t,g} - \sum_{g'=1}^{G} \frac{\Sigma_{s1,g' \to g}\phi_{g'}}{\phi_g} \tag{4}$$

In Equation (4) ϕ_g is scalar flux in group g and $\Sigma_{s1,g' \to g}$ is the P_1 cross section of scattering from group g' to group g.

Actually according to P_1 theory, the in-scatter can be treated exactly with given multi-group cross sections. In recent research on transport correction for hydrogen [10], a 70-group library for ^{1}H bound in water molecules was generated using NJOY [11], including a 70-group P_0 and P_1 scattering matrix with thermal scattering effect (using $s(\alpha, \beta)$ tables for light water molecules). Using the group data, the multi-group P_1 equations can be solved numerically to get the results of flux and current spectrum. Then transport cross section can be computed directly following the definition as

$$\Sigma_{tr,g}^{in} = \Sigma_{t,g} - \sum_{g'=1}^{G} \frac{\Sigma_{s1,g'\to g}\vec{J}_{g'}}{\vec{J}_g} \tag{5}$$

in which $\Sigma_{tr,g}^{in}$ is the transport cross section with in-scatter calculated directly and the result of this method will be used as reference for comparison with other approximation methods.

1.3. A Comparison among Different Approximation Methods

To get a sense of the performance of different approximation methods mentioned in the previous Section 1.2, a simple model with pure hydrogen uniformly distributed in infinite medium can be used as a test problem. The results of transport cross sections $\Sigma_{tr,g}$ and diffusion coefficients D_g computed from the three approximation methods, including the out-scatter (os) approximation, the asymptotic (as) approximation and the flux-limited (fl) approximation are compared with those from the in-scatter (in) method. The ratios of $\Sigma_{tr,g}$ to $\Sigma_{t,g}$ for different group structures in 2/4/10/70 groups are plotted in Figure 1.

In the 70-group and 10-group cases the flux-limited approximation method can match the in-scatter results well in the high energy and thermal range, but deviates obviously for the middle energy range from 100 eV to 1 MeV. While the out-scatter approximation fails to match in high energy range and the asymptotic method only work for a small energy range. When it comes to few groups such as 4 groups or 2 groups, all of the approximation methods have a big deviation from the reference results. A more direct comparison of diffusion coefficients in 4 and 2 groups is illustrated in Figure 2. In the cases of 4 groups and 2 groups, all of the diffusion coefficients of group 1 from the approximation methods have a deviation as big as 40% lower than the reference results.

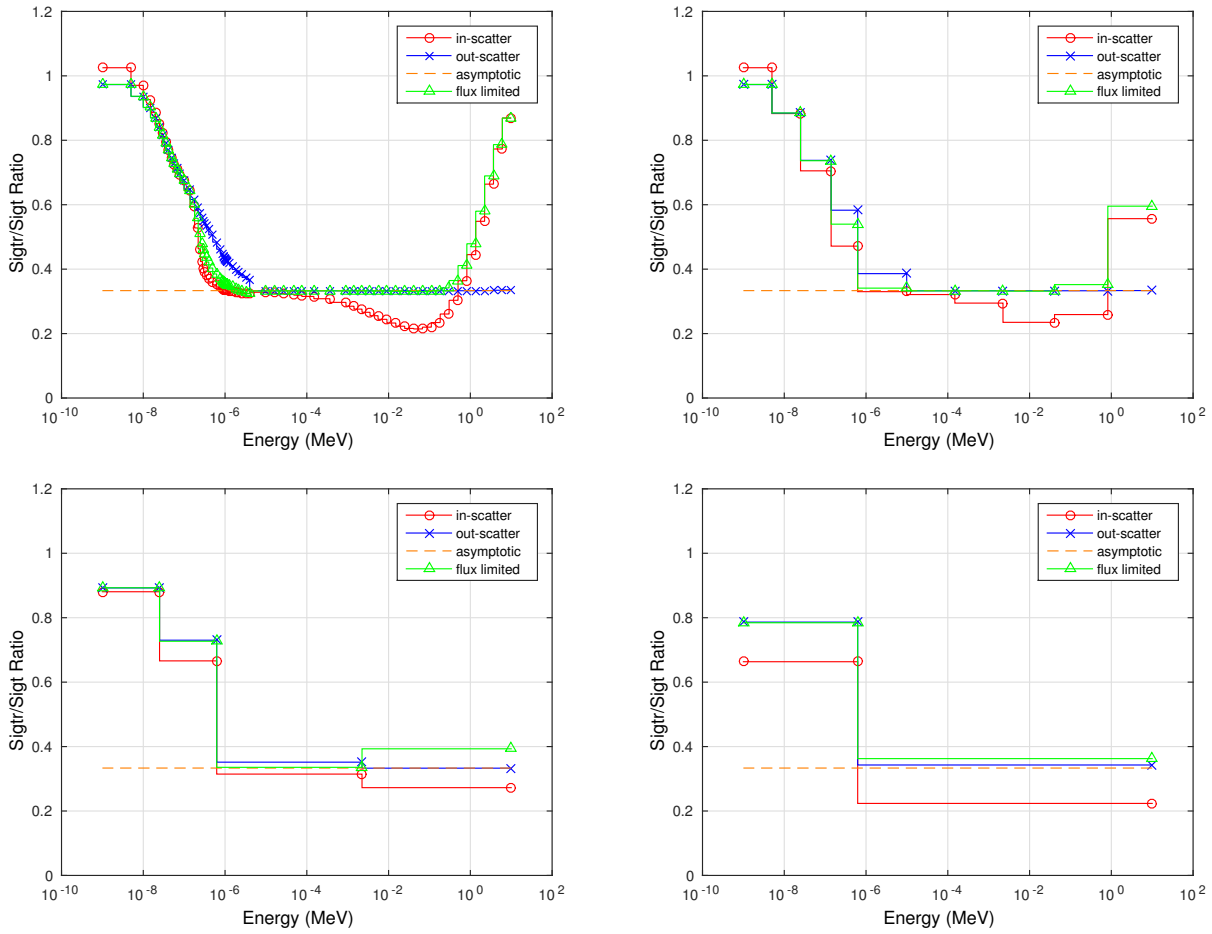

Figure 1. Comparison of multi-group ratio of $\Sigma_{tr,g}$ to $\Sigma_{t,g}$. (Upper-left: 70 groups; upper-right: 10 groups; bottom-left: 4 groups; bottom-right: 2 groups.)

2. ANALYTICAL DERIVATION AND NUMERICAL RESULTS OF TRANSPORT CORRECTION RATIO

2.1. Analytical Derivation of Transport Correction Ratio

The analytical transport correction ratio for an isotope with atomic mass A can be derived in infinite homogeneous medium with the assumption of only down scatter. In this case the diffusion coefficient can be derived from the second P_1 equation [12], as shown in Equation (6).

$$D(E) = \frac{1}{3\Sigma_t(E)}\left[1 + \frac{3}{\phi(E)}\int_E^{\frac{E}{\alpha}} \Sigma_{s1}(E' \to E)D(E')\phi(E')dE'\right] \tag{6}$$

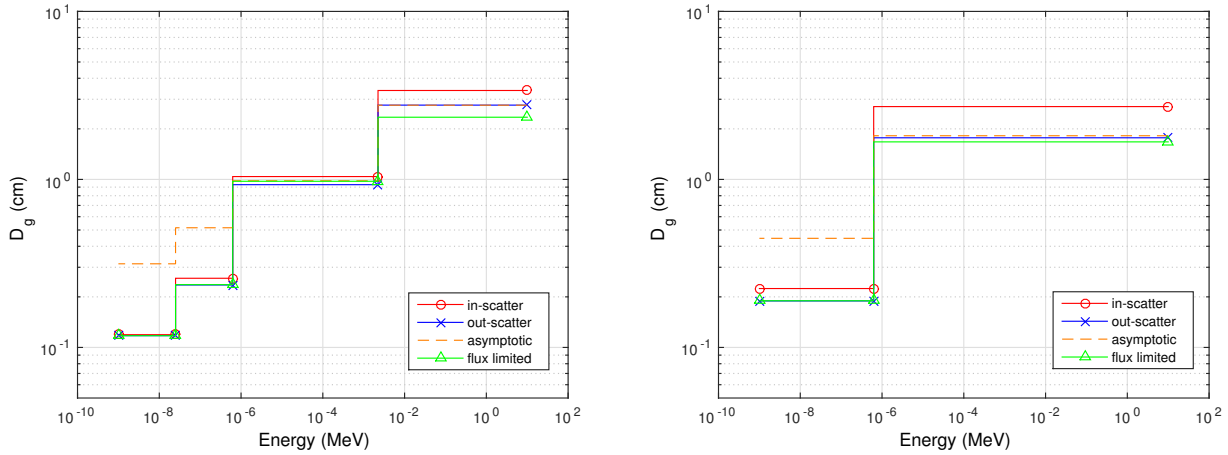

Figure 2. Comparison of multi-group diffusion coefficients D_g. (Left: 4 groups; right: 2 groups.)

In Equation (6) $\alpha = (A-1)^2/(A+1)^2$. The differential P_1 scattering cross sections can be expressed as

$$\Sigma_{s1}(E' \to E) = \bar{\mu}\frac{\Sigma_t(E')}{(1-\alpha)E'} = \frac{2}{3A}\frac{\Sigma_t(E')}{(1-\alpha)E'}. \tag{7}$$

Through the relationship between diffusion coefficient and transport cross section $D = 1/(3\Sigma_{tr})$, Equation (6) can be re-written as

$$\frac{1}{3\Sigma_{tr}(E)} = \frac{1}{3\Sigma_t(E)}\left[1 + \frac{3}{\phi(E)}\int_E^{\frac{E}{\alpha}} \frac{2}{3A}\frac{\Sigma_t(E')}{(1-\alpha)E'}\frac{1}{3\Sigma_{tr}(E')}\phi(E')dE'\right] \tag{8}$$

The transport correction ratio is defined as $f(E) = \frac{\Sigma_{tr}(E)}{\Sigma_t(E)}$. The ratio can be derived as Equation (9) by rearranging Equation (8) .

$$f(E) = \left[1 + \frac{2}{3A(1-\alpha)\phi(E)}\int_E^{\frac{E}{\alpha}} \frac{\phi(E')}{f(E')E'}dE'\right]^{-1} \tag{9}$$

According to slowing down theory, flux density at energy E can be approximated as

$$\phi(E) = \int_E^{E_{max}} \frac{\chi(E')}{\xi\Sigma_s(E')E'}dE' \tag{10}$$

in which $\chi(E')$ is the source density at energy E' from Watt fission spectrum, and $\xi = 1 + \frac{\alpha}{(1-\alpha)ln(\alpha)}$.

It should be noted that in the expression in Equation (9) $f(E)$ is dependent on the integration of $f(E')$, so before solving for $f(E)$ numerically, the value of $f(E_{max})$ should be set to unity based on the physical meaning of transport correction. The analytical result of transport correction ratio is computed by solving Equation (9) numerically and compared with the methods in Section 1.2 in Figure 3. The analytical result is not expected to match the in-scatter method perfectly for the approximated flux density in Equation (10), but the two results show consistent trend over energy, especially for the decreasing part before reaching the asymptotic ratio of $1/3$.

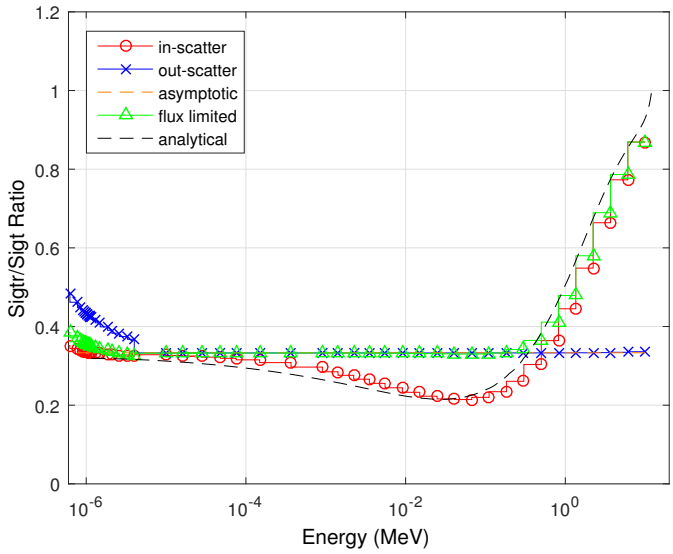

Figure 3. Comparison of multi-group transport correction ratio by approximation methods $VS.$ analytical result in down scatter energy range.

3. CUMULATIVE MIGRATION METHOD FOR DIFFUSION COEFFICIENTS

3.1. Theory of Migration Area

In diffusion theory [2], migration area is defined as in Equation (11) and can be proved to be equal to one-sixth of the average square of the flight distance from the position where a fast neutron is born to the position where it is absorbed as a thermal neutron.

$$M^2 = L^2 + \tau_{th} \tag{11}$$

In Equation (11) M^2 is migration area, L^2 is diffusion area and τ_{th} is neutron age of fast neutrons to thermal. Diffusion area is defined as

$$L^2 = \frac{D}{\Sigma_a} \tag{12}$$

where D is diffusion coefficient and Σ_a is absorption cross section.

Essentially τ_{th} is equal to one-sixth of the average square of the flight distance from the position where a fast neutron is born to the position where it is moderated to a thermal neutron, and L^2 is equal to one-sixth of the average square of the flight distance from the position where a neutron becomes thermal to the position where it is finally absorbed.

3.2. Multi-group Form and Cumulative Group Quantities

The definition of diffusion area in Equation (12) is considering a neutron from the position where it becomes thermal, in which case absorption is the only cause for the neutron's disappearance when regarding the thermal energy range as a single group. Similarly, if analyzing from the position where the fast neutron is originally born to the position where it is removed from a given energy range, in other words, the "partial" migration area when the neutron's energy is higher than a certain value E_0, the equation will also be justified as

$$M^2(E > E_0) = \frac{D(E > E_0)}{\Sigma_r(E > E_0)} \tag{13}$$

in which $M^2(E > E_0)$ is the cumulative migration area before the neutron's energy becomes lower than E_0, $D(E > E_0)$ is the diffusion coefficient for the energy range of $[E_0, E_{max}]$, and $\Sigma_r(E > E_0)$ is the removal cross section for the energy range of $[E_0, E_{max}]$, which will include not only absorption, but also net down scatter to a energy lower than E_0.

Actually from the perspective of energy group, the energy range of $[E_0, E_{max}]$ can be seen as a "broad" group whose top boundary always starts from E_{max}. In a multi-group structure, if E_0 is the bottom boundary of group g, then the "broad" group can be seen as a "cumulative group" from group 1 to group g. The concept of cumulative group is illustrated in Figure 4, in which the group structure is shown in a pyramid frame with cumulative group g and cumulative group $(g + 1)$ shown in shadowed parts. Based on this concept, Equation (13) can be re-expressed in the form of cumulative group as

$$(M_g^c)^2 = \frac{D_g^c}{\Sigma_{r,g}^c} \tag{14}$$

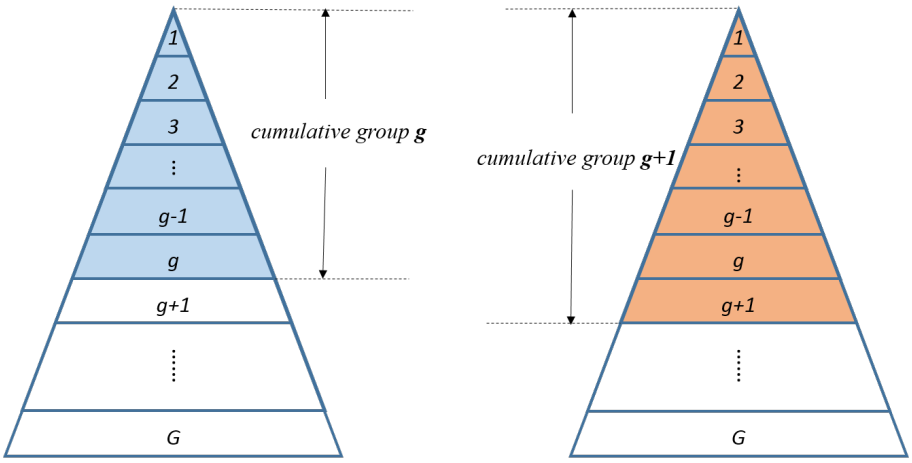

Figure 4. Illustration of the concept of "cumulative group". (Left: cumulative group g, right: cumulative group $(g+1)$.)

where the superscript c indicates that all the quantities in this equation are for the cumulative group g, that is to say, the "broad" group from group 1 to group g.

Equation (14) provides a scheme for computing cumulative multi-group diffusion coefficients through the theory of cumulative migration area, using the one-sixth relationship with the average square of neutron's flight distance, as shown as

$$(M_g^c)^2 = \frac{1}{6}\overline{(r_g)^2} \tag{15}$$

where r_g is the distance from the position where the neutron is originally born to the position where it is removed out of the cumulative group g, which is a quantity can be tallied directly in MC code. Then group-wise diffusion coefficients D_g can be backed out by "unfolding" cumulative multi-group diffusion coefficients D_g^c using flux-weighting as shown in Equation (16).

$$D_g^c = \frac{\sum_{g'=1}^{g} D_{g'}\phi_{g'}}{\sum_{g'=1}^{g} \phi_{g'}} \tag{16}$$

4. IMPLEMENTATION OF CUMULATIVE MIGRATION AREA TALLY IN OPENMC

In recent years, with the advance in computer technology, it has been investigated widely to utilize MC codes for generating homogenized lattice few-group cross section data for deterministic full core simulation, such as MCNP [13], Serpent [14], etc. In Serpent, firstly a continuous-energy Monte Carlo simulation is run to produce micro-group cross sections for B_1 equations, then the B_1 equations need to be solved for critical spectrum, which will be used to re-homogenize the cross sections into leakage-corrected few-group constants. The generation of micro-group cross sections needs more tally and computation work, which will make this method computationally inefficient.

In the homogenized few-group cross section data, the method for generating reliable diffusion coefficients poses a major challenge for the implementation in MC codes, since a rigorous theory for computing diffusion coefficients and transport cross sections is yet to be developed. Based on the theory in Section 3, the implementation scheme in OpenMC [15] is introduced in this section.

4.1. Tally Scheme for Cumulative Migration Area

In the implementation of the Cumulative Migration Method (CMM) for computing multi-group diffusion coefficients and transport cross sections in OpenMC, the crucial tally is cumulative migration area. The main events that change neutrons' energy and flight path is scatter, while the loss of neutrons is mainly resulted from absorption. Both down and up scatter should be taken into account in the cumulative migration area tally.

The tally scheme for cumulative migration area $(M_g^c)^2$ and cumulative number of neutrons tallied N_g^c in one reaction (scatter or absorption) is shown in Figure 5. In the figure of flowchart, g is the group index of the neutron before a reaction, g' is the group index of the neutron after a scatter reaction, G is the total number of groups, and r^2 is the square of the distance from the neutron's birth position to the position of the reaction.

This tally scheme can be used for any group structure and scores can be tallied directly into the desired few group structure, which avoids additional micro-group tally for B_1 spectrum calculation as in Serpent. In the implementation only one more score of cumulative migration area $(M_g^c)^2$ is added to MC code, which enables it to be both flexible and computationally efficient.

4.2. Phantom Tracking in Finite Medium

The cumulative migration area is simple to tally in infinite medium, however, in practice most simulations with MC code are in finite geometry. Even though there are many simulations in infinite medium, the actual practice is using finite geometry with reflective boundary conditions. But according to the

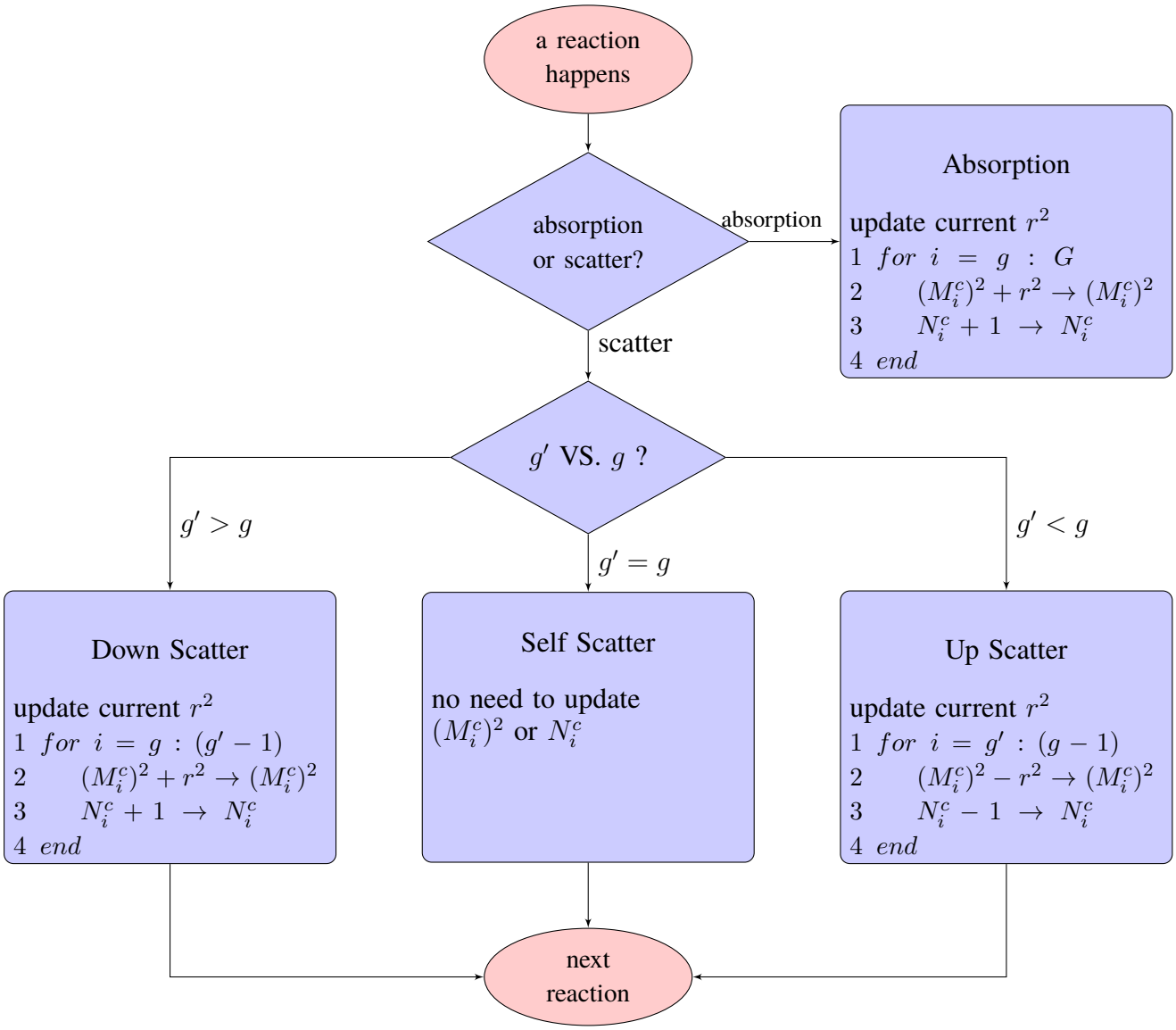

Figure 5. Flowchart of tally scheme for cumulative migration area $(M_g^c)^2$ and cumulative number of neutrons N_g^c for reactions of absorption and scatter.

theory of cumulative migration area, when a neutron undergoes a reflection on any reflective boundary, the actual position used in tally and computation should be the position as if there were no boundaries, which can be called the "phantom" position. Thus for problems with finite geometry and reflective boundary conditions, phantom tracking for neutrons should be established for the tally of cumulative migration area.

The phantom tracking for rectangular cuboid geometries has been implemented in OpenMC. The essential idea of the implementation is to utilize three $reflectionflags$ for each Cartesian axis, then the

flight direction as well as position of a neutron's phantom at any reaction can be inferred by these three flags. The cumulative migration area is tallied based on the positions of the phantom, instead of the real neutron.

5. SIMULATION RESULTS AND ANALYSIS

Several simulation problems has been completed using OpenMC with the added feature of computing diffusion coefficients and transport cross sections using CMM. In this section, the results of a simple problem of pure hydrogen and a real assembly from BEAVRS benchmark are presented.

5.1. Infinite Medium of Hydrogen

A simple problem of pure hydrogen in infinite medium is modeled and simulated for a comparison of the diffusion coefficients and transport cross sections computed using CMM and those of the in-scatter method in Section 1.3.

The model is built as a rectangular cuboid geometry with all reflective boundary conditions. According to the analysis of phantom tracking in Section 4.2, the cuboid can be in any size and will give the same results. In addition, the transport correction ratio should be independent of density of the problem, which has also been tested.

The simulation result is compared with in-scatter method in Figure 6. The transport correction ratio computed from OpenMC with CMM matched perfectly with in-scatter method, indicating that the transport cross section as well as diffusion coefficients from these two methods also agree very well. That is to say, CMM actually generates the same multi-group diffusion data as the data calculated directly by solving P_1 equations.

5.2. 2-group Diffusion Data for a BEAVRS Assembly

5.2.1. Configuration of the Assembly

To further evaluate the effect of the Cumulative Migration Method, it also has been used to generate 2-group diffusion data for a real assembly from BEAVRS benchmark [16]. The assembly simulated is the 2.4 wt-% ^{235}U with 12 burnable absorber pins, which recently has also been used by Serpent for computing 2-group constants [17]. The configuration of this assembly can be seen in Figure 7.

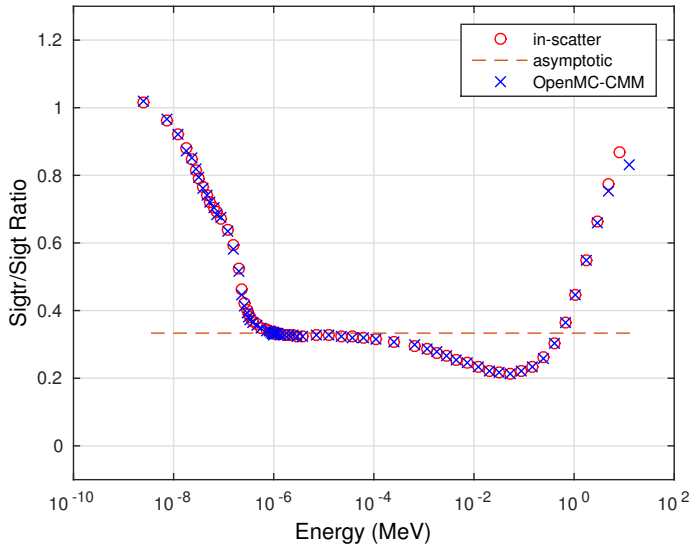

Figure 6. Comparison of 70-group transport correction ratio generated from OpenMC with Cumulative Migration Method (OpenMC-CMM) $VS.$ in-scatter method.

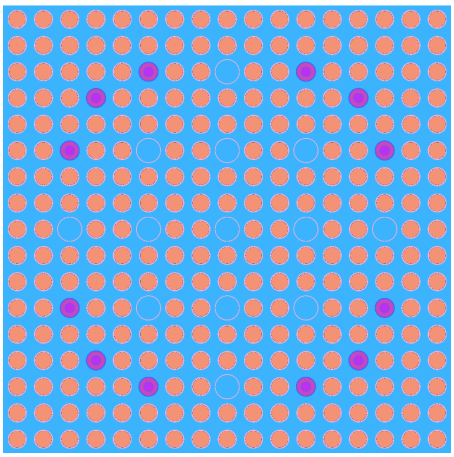

Figure 7. Configuration of the BEAVRS assembly of 2.4 wt-% ^{235}U with 12 burnable absorber pins.

5.2.2. 2-group Diffusion Data

The 2-group constants generated by OpenMC using CMM is compared with those generated by CASMO and Serpent as shown in Table I[1]. The group constants compared in the table include diffusion coeffi-

[1]For the results from Serpent and OpenMC, only the mean value of each parameter is listed in this table. The method of computing uncertainty for cumulative group quantities is to be investigated in ongoing research. The results from Serpent and OpenMC are computed with the same total number of neutrons.

cients (D_1, D_2), absorption cross sections (Σ_{a1}, Σ_{a2}), net-down scatter cross section ($\Sigma_{s,1\to2}$), fission neutron production cross sections ($\nu\Sigma_{f1}$, $\nu\Sigma_{f2}$), surface discontinuity factors (DF_1^s, DF_2^s) and k_{inf} calculated using the 2-group data. The 2-group data generated by OpenMC with CMM in Table I is closer to that of CASMO, especially for the diffusion coefficient of fast group.

Table I. 2-group constants for the BEAVRS assembly of 2.4 wt-% ^{235}U with 12 burnable absorber pins generated by CASMO, Serpent and OpenMC.

Parameter	Serpent	CASMO	OpenMC
D_1	1.397E+00	1.430E+00	1.426E+0
D_2	3.933E-01	3.775E-01	3.992E-1
Σ_{a1}	8.906E-03	8.908E-03	8.919E-3
Σ_{a2}	8.380E-02	8.297E-02	8.408E-2
$\nu\Sigma_{f1}$	5.343E-03	5.371E-03	5.380E-3
$\nu\Sigma_{f2}$	1.019E-01	1.009E-01	1.019E-1
$\Sigma_{s,1\to2}$	1.835E-02	1.804E-02	1.838E-2
DF_1^s	9.947E-01	9.931E-01	9.929E-1
DF_2^s	1.060E+00	1.061E+00	1.057E+0
k_{inf}	1.01469	1.01323	1.01281

6. CONCLUSION

The Cumulative Migration Method (CMM) for computing homogenized lattice multi-group diffusion data using Monte Carlo code is proposed in this paper. To overcome the shortcomings in various approximation methods for computing neutron transport cross sections and diffusion coefficients, which have been in use for more than 40 years, the theory of cumulative migration area and its relationship with transport cross sections and diffusion coefficients is developed for utilization to Monte Carlo tally schemes.

This method has been implemented in OpenMC and several test problems have been simulated for generating homogenized multi-group diffusion data. The results demonstrate that it is the P_1 diffusion coefficients, and not the B_1 diffusion coefficients, that are totally consistent with diffusion coefficients computed with CMM. This helps tremendously to settle the longstanding argument over the appropriateness of the P_1 and B_1 models of diffusion coefficients.

Another distinct advantage of CMM is that no where does one have to make provisions for lattices that have voids (many deterministic codes opt to spatially homogenize transport cross sections to avoid singularities caused by voids and the energy collapse one over sigma transport to obtain an accurate energy collapse). CMM handles void very naturally and no decisions are required regarding the proper energy collapse.

In addition, one of the most significant accomplishment of CMM is that few group diffusion coefficients and transport cross sections can be computed directly in the desired few group structure – without the necessity of tallying fine group cross sections that are currently employed in Monte Carlo B_1 or P_1 spectrum calculations. These few group diffusion coefficients are exactly the same as those that are tallied in fine energy group tallies and then collapsed to few groups. Consequently, CMM provides tremendous simplifications of the tallies needed in Monte Carlo to compute accurate homogenized lattice diffusion coefficients and transport cross sections.

ACKNOWLEDGMENTS

The research work presented in this paper was supported by the Idaho National Laboratory under DOE Idaho Operations Office Contract DE-AC07-05ID14517.

REFERENCES

[1] George I. Bell and Samuel Glasstone. *Nuclear Reactor Theory*. Robert E. Krieger Publishing Co., Huntington, NY, USA (1979).

[2] John R. Lamarsh. *Introduction to Nuclear Reactor Theory*. Addison-Wesley, Reading, MA, USA (1966).

[3] T. Newton and J. Hutton. "The next generation wims lattice code: Wims9." *Proceedings of New Frontiers of Nuclear Technology, PHYSOR*, (pp. 7–10) (2002).

[4] H. Huria *et al.* "Theory and methodology of westinghouse phoenix-h/anc-h for hexagonal pwr cores." *Transactions of the American Nuclear Society*, **71(CONF-941102–)** (1994).

[5] G. Marleau, R. Roy, and A. Hébert. "Dragon: a collision probability transport code for cell and supercell calculations." *Report IGE-157, Institut de génie nucléaire, École Polytechnique de Montréal, Montréal, Québec* (1994).

[6] E. A. Villarino *et al.* "Helios: angularly dependent collision probabilities." *Nuclear Science and Engineering*, **112(1)**: pp. 16–31 (1992).

[7] B. R. Herman *et al. Improved diffusion coefficients generated from Monte Carlo codes*. *Technical report*, American Nuclear Society, 555 North Kensington Avenue, La Grange Park, IL 60526 (United States) (2013).

[8] R. J. Stamm'ler and M. J. Abbate. *Methods of steady-state reactor physics in nuclear design*, volume 111. Academic Press London (1983).

[9] G. Pomraning. "Flux-limited diffusion theory with anisotropic scattering." *Nuclear Science and Engineering*, **86(4)**: pp. 335–343 (1984).

[10] B. R. Herman. *Monte Carlo and Thermal Hydraulic Coupling using Low-Order Nonlinear Diffusion Acceleration*. Ph.D. thesis, Massachusetts Institute of Technology, 77 Massachusetts Avenue, Cambridge, MA 02139, USA (2014).

[11] R. E. Macfarlane, D. Muir, and D. George. "Njoy99. 0 code system for producing pointwise and multigroup neutron and photon cross sections from endf/b data." *Los Alamos National Laboratory, PSR-480*, **7** (2000).

[12] A. Hebert. *Applied reactor physics*. Presses inter Polytechnique (2009).

[13] J. M. Pounders. "Stochastically generated multigroup diffusion coefficients." (2006).

[14] E. Fridman and J. Leppänen. "On the use of the serpent monte carlo code for few-group cross section generation." *Annals of Nuclear Energy*, **38(6)**: pp. 1399–1405 (2011).

[15] P. K. Romano and B. Forget. "The openmc monte carlo particle transport code." *Annals of Nuclear Energy*, **51**: pp. 274–281 (2013).

[16] N. Horelik *et al.* "Benchmark for evaluation and validation of reactor simulations (beavrs), v1. 0.1." In: *Proc. Int. Conf. Mathematics and Computational Methods Applied to Nuc. Sci. & Eng* (2013).

[17] J. Leppänen and R. Mattila. "On the practical feasibility of continuous-energy monte carlo in spatial homogenization." *PHYSOR* (2014).